LAWRENCE
LIVERMORE
NATIONAL
LABORATORY

LLNL-PROC-401213

A Detailed Chemical Kinetic Reaction Mechanism for Oxidation of Four Small Alkyl Esters in Laminar Premixed Flames

C. K. Westbrook, W. J. Pitz, P. R. Westmoreland, F. L. Dryer, M. Chaos, P. Osswald, K. Kohse-Hoinghaus, T. A. Cool, J. Wang, B. Yang, N. Hansen, T. Kasper

February 11, 2008

International Symposium on Combustion
Montreal, Canada
August 3, 2008 through August 8, 2008

Disclaimer

A Detailed Chemical Kinetic Reaction Mechanism for Oxidation of Four Small Alkyl Esters in Laminar Premixed Flames

C. K. Westbrook[1], W. J. Pitz[1],
P. R. Westmoreland[2],
F. L. Dryer[3], M. Chaos[3],
P. Osswald[4], K. Kohse-Hoinghaus[4],
T. A. Cool[5], J. Wang[5], B. Yang[5],
N. Hansen[6] and T. Kasper[6]

1 Lawrence Livermore National Laboratory, Livermore, CA, USA
2. University of Massachusetts, Amherst, MA, USA
3. Princeton University, Princeton, NJ, USA
4. Bielefeld University, Bielefeld, Germany
5. Cornell University, Ithaca, NY, USA
6. Sandia National Laboratories, Livermore, CA, USA

Corresponding Author:

Dr. Charles K. Westbrook
Lawrence Livermore National Laboratory
P. O. Box 808
7000 East Avenue
Livermore, CA 94550 USA

westbrook1@llnl.gov

Paper length: 5780 words
Main text: 3689 using Microsoft Word Count utility
References: 385 (20 references +2) x (2.3 lines/reference)x(7.6 words/line)
Table: 100 (45 mm x 2.2 words/mm)
Figure 1: 169 (63 mm + 10) x 2.2 + 8 words in caption
Figure 2: 111 (35 mm + 10) x 2.2 + 12
Figure 3: 134 (40 mm + 10) x 2.2 + 24
Figure 4 : 293 (115 mm + 10) x 2.2 + 18
Figure 5 : 303 (115 mm + 10) x 2.2 + 28
Figure 6 : 303 (115 mm + 10) x 2.2 + 28
Figure 7 : 293 (115 mm + 10) x 2.2 + 18

Colloquium : Laminar Flames

Supplemental material is available for this paper

A Detailed Chemical Kinetic Mechanism for Oxidation of Four Small Alkyl Esters in Laminar Premixed Flames

C. K. Westbrook[1], W. J. Pitz[1],
P. R. Westmoreland[2],
F. L. Dryer[3], M. Chaos[3],
P. Osswald[4], K. Kohse-Hoinghaus[4],
T. A. Cool[5], J. Wang[5], B. Yang[5],
N. Hansen[6] and T. Kasper[6]

1 Lawrence Livermore National Laboratory, Livermore, CA, USA
2. University of Massachusetts, Amherst, MA, USA
3. Princeton University, Princeton, NJ, USA
4. Bielefeld University, Bielefeld, Germany
5. Cornell University, Ithaca, NY, USA
6. Sandia National Laboratories, Livermore, CA, USA

Abstract

A detailed chemical kinetic reaction mechanism has been developed for a group of four small alkyl ester fuels, consisting of methyl formate, methyl acetate, ethyl formate and ethyl acetate. This mechanism is validated by comparisons between computed results and recently measured intermediate species mole fractions in fuel-rich, low pressure, premixed laminar flames. The model development employs a principle of similarity of functional groups in constraining the H atom abstraction and unimolecular decomposition reactions in each of these fuels. As a result, the reaction mechanism and formalism for mechanism development are suitable for extension to larger oxygenated hydrocarbon fuels, together with an improved kinetic understanding of the structure and chemical kinetics of alkyl ester fuels that can be extended to biodiesel fuels. Variations in concentrations of intermediate species levels in these flames are traced to differences in the molecular structure of the fuel molecules.

Keywords: Reaction mechanisms, laminar flames, oxygenates

1. INTRODUCTION

Concerns about long-term availability of conventional petroleum-based fuels, the continuing need to reduce harmful emissions of atmospheric pollutants, and the urgency of reducing emissions of greenhouse gases are all creating interest in various types of renewable biofuels. One important class of biofuels consists of large methyl and ethyl esters derived from vegetable and other oils [1]. These biofuels operate well in diesel and HCCI engines, with another attractive feature that the oxygen atoms imbedded within the biodiesel fuel molecule help reduce soot production from diesel engines [2,3].

While an enormous number of kinetic studies have been published on the subject of hydrocarbon kinetics, few experimental or kinetic modeling studies have been carried out for alkyl ester molecules, which severely limits our ability to predict their combustion properties, such as heat release rates, amounts of pollutant emissions, types and levels of intermediate species, or ignition properties. Most practical biodiesel fuel molecules, including soy and rapeseed biodiesel fuel, are methyl esters with as many as 16 - 18 carbon atoms in the form of a long, straight chain, either saturated or with some double bonds in the long chain. The large size of such molecules has been an impediment to the development of detailed kinetic models for them. A recent study describes a detailed kinetic model for methyl decanoate [4], a large methyl ester with a carbon chain containing ten C atoms, and several other recent kinetic modeling studies [5-9] have examined the kinetics of small methyl and ethyl esters with chains of 2 to 4 carbon atoms. The present work is part of a systematic approach towards a better kinetic understanding of methyl and ethyl ester fuels, focusing attention on the kinetic description of the essential ester portion of such fuel molecules and showing how that ester moiety

influences the rate of combustion of the hydrocarbon portions of those fuels. Our intent is to reduce the complexity associated with large biodiesel fuels by combining detailed experimental and kinetic modeling studies of low pressure, fuel-rich, laminar, premixed flames with four different small alkyl ester fuels. Models for combustion chemistry of small molecule analogs for larger biodiesel molecules will then be valuable in developing models for larger, full-size biodiesel molecules.

Historically, validations of detailed kinetic models have emphasized simulations of homogeneous environments such as shock tubes or rapid compression machines, but simulations of laminar flame speeds have not been very useful as validation tests. However, current experiments are now able to quantify spatial variations in mole fractions of many reactant, product and intermediate species, including some radicals, within low pressure flames, all of which are much more demanding tests of kinetic models than are laminar burning velocities, representing an important advance in the type of experimental tools available for kinetic research.

2. FUELS STUDIED AND KINETIC REACTION MECHANISMS

Four very similar small methyl and ethyl ester fuels were used in the present study, consisting of methyl formate ($C_2H_4O_2$, m/z = 60), methyl acetate ($C_3H_6O_2$, m/z = 74), ethyl formate ($C_3H_6O_2$, m/z = 74) and ethyl acetate ($C_4H_8O_2$, m/z = 88). Spatial variations in mole fractions of 28 different stable and radical species for the m/z = 74 structural isomers methyl acetate and ethyl formate were reported by Osswald et al. [10], and spatial profiles for the other two fuels have been measured by the same experimental group [11]. Osswald et al. [10] discussed possible reaction pathways and their relationships with structures for methyl acetate and ethyl formate, although no kinetic modeling was carried out.

Few detailed kinetic mechanisms have been reported for any of these fuels. Several kinetic mechanisms for a larger methyl ester, methyl butanoate ($C_5H_{10}O_2$, m/z = 102) have been developed [5-7,12], in part to see if methyl butanoate could be useful as a surrogate for modeling biodiesel combustion. In addition, Metcalfe et al. [7] developed a detailed kinetic mechanism for high temperature oxidation of ethyl propanoate ($C_4H_8O_2$, m/z = 88), a structural isomer of ethyl acetate.

Dagaut et al. [9] studied methyl acetate oxidation in a jet-stirred reactor and developed a kinetic mechanism, largely based on structural similarities between methyl acetate and related species including methanol, dimethyl ether, and ethane. Gasnot et al. [8] developed a detailed kinetic oxidation mechanism for ethyl acetate, with submechanisms for vinyl acetate and acetic acid, to study stoichiometric methane/air flames with additions of 1, 2 and 3% ethyl acetate. They also employed similarities between ethyl acetate and other species to build their detailed kinetic mechanism. Good

and Francisco [13] carried out an extensive analysis of methyl formate and dimethyl ether oxidation, using ab initio techniques, to provide kinetic insights into important reaction pathways for methyl formate oxidation.

The present kinetic modeling study uses a similar approach to develop detailed mechanisms for these small ester species, but the goal is to produce a single, internally self-consistent mechanism for all of these alkyl ester fuels that emphasizes their structural similarities. In addition to the present four flames, this mechanism then provides a base and set of kinetic rules on which to build mechanisms for larger esters in future experimental studies.

The four ester fuels of this study are shown schematically in Figure 1, illustrating their strong structural similarities. All have the central -O(C=O)- group, and each has either a methyl or ethyl group attached to the O atom and either an H atom (in the formates) or methyl radical (in the acetates) bonded to the C=O structure; these structural similarities have been exploited in the construction of the present mechanism.

Consumption of these ester fuels is accomplished via unimolecular decomposition and abstraction of individual H atoms by radical species. Rates of both fuel consumption pathways depend in predictable ways on the structure of the fuel molecule, and especially on the strength of the bond being broken. Bond strengths depend on electronic structure in the vicinity of that bond, so in practical terms, they depend on the identities of the neighboring atoms close to the bond being broken.

Figure 1 shows that the ethyl groups in ethyl formate and ethyl acetate have C-H bond strengths that are close to identical, since both have CH_2 groups that are bonded to identical methyl and -O(C=O)- groups, and their CH_3 groups are bonded to identical

-$CH_2O(C=O)$- groups. Therefore, we have assumed that H atom abstraction reactions from these ethyl groups have identical rates with each radical reactant. The same logic applies to abstraction reactions of the formate group H atom in methyl formate and ethyl formate, and to the abstraction reactions of H atoms from the acetate groups in methyl acetate and ethyl acetate. Preliminary H atom abstraction rates were estimated based on reactions in molecules with similar molecular structures, and then revised by comparisons with experimental results as described below.

For methyl acetate and methyl formate, unimolecular decomposition initiation reactions involve breaking a C-O bond to produce methyl or methoxy radicals. However, for ethyl esters, another unimolecular elimination reaction producing ethene is also observed, via a six-membered transition state ring, with a rate rapid enough to contribute significantly to fuel consumption. These reactions are shown schematically in Figure 2, showing that analogous reactions in methyl acetate and methyl formate must proceed through a more strained 5-membered transition state ring, with a correspondingly much lower rate. Consistent with this analysis, Metcalfe et al. [7] observed that ethyl propanoate ignited much more rapidly in shock tube conditions than its structural isomer, methyl butanoate, because ethyl propanoate was consumed by a rapid ethene molecular elimination reaction like those in Fig. 2, while methyl butanoate, like methyl acetate and methyl formate in the present study, did not have such a rapid molecular elimination reaction. Since the transition states for both ethene elimination reactions are the same in the ethyl esters, the rates of both initiation reactions are assumed to be equal, with an activation energy of 50 kcal/mol equal to that for ethyl propanoate [14], and an A-factor of 1.0×10^{13} close to the value of 4.0×10^{12} estimated by O'Neal and Benson [15].

3. EXPERIMENTS

A flame-sampling molecular-beam mass spectrometer, employing tunable vacuum-ultraviolet synchrotron radiation for photoionization was used to study these premixed, low-pressure (30 Torr) flat flames [10]. The essential features include a low-pressure flame chamber, a differentially pumped molecular-beam flame-sampling system, and a linear time-of-flight mass spectrometer (TOFMS), coupled to a 3-m monochromator used to disperse synchrotron radiation at the Advanced Light Source of the Lawrence Berkeley National Laboratory. Flame gases are sampled by a quartz cone along the axis of the flat flame burner, and the burner can be moved toward or away from the sampling cone to make measurements at different distances within the flame.

A molecular beam from the sampling system is then crossed by the dispersed VUV light from the monochromator, and photoions are collected and mass-analyzed with a TOFMS with a mass resolution of $m/\Delta m = 400$ and finally converted into spatial profiles of specific chemical species. The experiments can discriminate between isomers at many mass numbers, based on differences in ionization energies, although some combinations of signals are very difficult to separate when their ionization energies are very similar. Osswald et al. [10] estimated the experimental uncertainties in major species as $\pm$15-20%, most intermediate species as $\pm$30-40% and radical species as uncertain by factors of 2-4.

Flame temperatures were measured in separate experiments at Bielefeld University using laser-induced fluorescence (LIF) of seeded NO (0.5%). The LIF measurements were carried out under flame conditions unperturbed by the sampling cone,

and the "distance from the burner" used by Osswald et al. [10] and in this study is taken to be 0.9 mm (4.5 sampling orifice diameters) less than the actual separation between the burner and the tip of the sampling cone to account approximately for the probe sampling gases slightly upstream of the sample orifice [10]. Temperature profiles have not yet been completely characterized for the methyl formate and ethyl acetate flames, so temperature values used for these flames are the same as those in the similar methyl acetate flame. Sensitivity studies showed that the computed intermediate chemical species profiles are not very sensitive to minor changes in the temperature profiles assumed for these flames.

4. COMPUTED RESULTS

Flame models were computed for the four ester flames, using the Chemkin 4.0 software [16]. Transport parameters for ester fuels and their intermediate species were estimated from species of similar size and structure for which parameters were available. A mixture averaged transport model was used in the flame calculations. A minimum of 200 computational zones were used to ensure sufficient resolution of each flame. Inlet flow conditions for each flame are summarized in Table 1. All four flames are fuel-rich and diluted by argon, and in each model calculation, the spatial temperature was specified, so the energy equation was not solved in the Chemkin simulation.

An initial reaction mechanism was prepared for each of these fuels, built on a recent C_1-C_4 mechanism from Curran et al. [17]. A kinetic submechanism for acetic acid, a major product of ethyl acetate consumption, was taken from Gasnot et al. [8] and included here. Computed species profiles were then compared with experimental values, with mixed initial results. Sensitivity analysis and reaction path analysis were used to modify the reaction rate parameters to arrive at an optimized set of rate parameters. The only reaction rate parameters directly involving the ester fuel molecules with significant sensitivities were H atom abstraction reactions with H, OH and HO_2 and the unimolecular decompositions, but the most significant sensitivities involved the different reaction pathways available for each fuel, following H atom abstractions at different sites in the fuel molecule, as discussed below. For each flame, the major species CO, CO_2, H_2, H_2O, O_2 and fuel were reproduced very well, as illustrated for the methyl formate flame in Figure 3.

4.1 Methyl acetate

Methyl acetate (MA) contains two different methyl radicals, each with somewhat different C-H bond strengths, and different model compounds were used to estimate H atom abstraction rates. Rates of H atom abstractions from the methyl radical bound to the O atom in the ester group were taken from the structurally similar methyl radical in methyl butanoate [5,6]. The other methyl in methyl acetate is influenced by the adjacent C=O group and has a C-H bond energy (97.7 kcal/mol [14]) similar to that for the tertiary C-H bond in methyl cyclohexane (96.5 kcal/mol) [18], which was used as the initial model compound. Abstractions from the two methyl groups lead to different intermediate species. The $\bullet CH_2O(CO)CH_3$ (Path 1) radical decomposes via β-scission to produce formaldehyde and acetyl, and the acetyl rapidly decomposes to produce methyl and CO, although a small percentage of the acetyl radicals recombine with methyl radicals to produce acetone. In contrast, the $CH_3O(CO)H_2C\bullet$ (Path 2) radical decomposes to produce ketene and the methoxy radical. The methoxy radical can produce methanol by abstracting another H atom from the fuel, recombine with methyl to produce dimethyl ether, or decompose to produce formaldehyde and H atoms. Ethene is produced only via methyl/methyl recombination followed by ethane dehydrogenation. Thus Path 1 produces all of the acetone and most of the formaldehyde in this flame, while Path 2 produces all of the ketene and dimethyl ether, and both paths lead to relatively small levels of ethene.

The initial reaction rates were found to produce high levels of ketene and dimethyl ether, but reasonably accurate levels of most of the other intermediate species. The H atom abstraction rates for Path 2 were all therefore reduced, simply by reducing

the A factors by a factor of almost 10 in each rate expression, leading to the computed results shown in Figures 4-7 for the MA flame. The Path 1 H abstraction reaction rates produced excellent agreement for intermediate species predictions without further modification, confirming that the use of rates from the same structural group in methyl butanoate can be transferred intact to methyl acetate with very good accuracy. Use of Path 2 reaction rates from a methyl radical in a differently structured molecule introduced errors that required corrections based on comparisons with experimental results.

4.2 Ethyl formate

The same approach was used for initial H atom abstraction rates in ethyl formate (EF). Rate expressions for H atom abstraction producing n-propyl and iso-propyl radicals from propane [17] were used as the initial estimates of analogous reaction rates of the ethyl radical in EF. Similarly, H atom abstraction rates in the weak C-H bond in the formate part of EF were estimated based on secondary H atom abstractions in methyl cyclohexane [18].

As with MA, different H atom abstraction paths in EF produce different intermediate species. The primary H atom abstraction Path 3 produces ethene and CO_2, the secondary H atom abstraction Path 4 produces acetaldehyde and CO, and the formate H abstraction Path 5 produces CO_2 and ethyl, which rapidly produces ethene. Computed results with the initial EF submechanism predicted levels of methane, acetaldehyde and formaldehyde too high by factors of 2-4, while predictions of ethene, ketene, and acetylene were too low by similar factors. Best overall agreement between the computed and experimental mole fraction profiles was found when rates for H abstractions via Path

3 were increased by a factor of 2, those for Path 4 were decreased by a factor of 4, and those for Path 5 decreased by a factor of 2, with those results shown for selected species in Figures 4 through 7. The need for these rate adjustments reflects the fact that the C-H bonds in the different model compounds are different from those in ethyl formate.

4.3 Ethyl acetate and methyl formate

Ethyl acetate and methyl formate contain the same functional groups as ethyl formate and methyl acetate, all based on a central -O(C=O)- group, but with the ethyl and methyl groups interchanged. Therefore, the initial submechanisms for ethyl acetate and methyl formate assumed that the H atom abstraction rates in each of the functional groups are exactly the same as those in the first pair of fuels. The subsequent decomposition products of each radical in ethyl acetate and methyl formate are different from the analogous radicals in ethyl formate and methyl acetate, and comparisons between computed and experimental species profiles must show whether or not the similarities in H abstraction rates can be translated into accurate predictions of intermediate species.

There are three H atom abstraction pathways in ethyl acetate, originating with abstraction of the primary H atom (Path 6) and the secondary H atom (Path 7) in the ethyl group and the acetyl H atom (Path 8) from the acetyl group. Path 6 produces ethene as its most important signature, Path 7 produces acetyl radicals and stable acetaldehyde, and Path 8 produces ketene and the ethoxy radical.

Similarly, there are two H atom abstraction pathways in methyl formate, the first being the methyl group and the second consisting of the formate H atom bonded to the

C=O group. Abstraction of an H atom from the methyl group (Path 9) leads to formaldehyde and a formyl radical, while abstraction of the formate H atom (Path 10) produces methyl and CO_2.

Comparisons between computed and experimentally measured intermediate species concentrations are shown for selected species in Figures 4-7 for the initial families of H atom abstraction rates, with overall excellent agreement. Subsequent optimizations produced very minor changes in the overall agreement between the computed and experimental results. The final rate expressions are for all four ester fuels are provided as supplementary material in Table S1.

These results for H atom abstraction rates should not be surprising. The electronic structure and C-H bond strengths in the $CH_3CH_2O(C=O)$- group are not very different when the final group is an H atom or a methyl radical, so the abstraction rates should be nearly equal. Confirmation is provided by a recent theoretical study by Sumathi and Green [19] who found that secondary C-H bond strengths in the ethyl radical part of ethyl formate and ethyl acetate differ by only 0.3 kcal/mol. The same similarities exist for the C-H bond strengths in the $CH_3O(C=O)$- group and for the -$O(C=O)H$ and -$O(C=O)CH_3$ groups, again in good agreement with theoretical results of Sumathi and Green, and the excellent overall agreement in the present results confirms this view.

5 DISCUSSION

Figure 4 shows the mole fractions of the C_2 species, ethene and acetylene, in the four flames. The EA and EF flames produce much higher levels of these species, since

ethene is produced directly from the ethyl groups, while the MA and MF fuels must produce C_2 species by methyl recombination followed by dehydrogenation. Acetylene peaks farther from the burner than ethene in both experiments and model calculations, consistent with the fact that acetylene is produced from ethene, and the peak values of acetylene are lower than peak ethene levels except in the experimental MA flame results.

Figure 5 shows the same type of relationship between formaldehyde and formyl radical in all four flames, with peak formyl values following those of its parent formaldehyde. Absolute levels of both species are in excellent agreement between experimental and computed values. In contrast with the C_2 species, the MA and MF flames produce much higher levels of formaldehyde than the ethyl esters, since formaldehyde is an immediate β-scission product from H atom abstraction from the methyl group.

The products of H atom abstraction from the acetate group, followed by β-scission, can be seen from Figure 6, showing much higher ketene levels from EA and MA than from the formates. The acceptable agreement between computed and measured levels of propyne suggest that the reaction mechanisms can be extended to future studies of soot formation from ester fuels, and the relative amounts of propyne production reflect the importance of C_2 species in propyne formation and soot production.

Methane is produced as a major intermediate in all four flames from methyl radicals that abstract H atoms from the fuel, and the excellent agreement between computed and measured levels of methane in Figure 7 indicates that the methyl radical values are being predicted accurately. Acetaldehyde production follows a variety of rather complicated pathways in these flames, directly in the EA flame and by H atom

abstraction by acetyl radicals in the EA and MA flames. Agreement between computed and experimental values is very good and provides additional validation of the kinetic mechanisms.

Finally, experimental results for a considerable number of species for all four flames in Fig. 4-7 show high values at locations near the burner that cannot be reproduced by the kinetic models. These differences suggest possible kinetic effects in or on the surface of the burner, or difficulties of making species measurements very close to the burner where the sampling cone may disturb the flows.

One goal of the present work is to establish a core kinetic reaction mechanism for methyl and ethyl esters of increasing complexity. We have noted above that the methyl group H atom abstraction reaction rates in methyl butanoate [5-7] were used without change in the present methyl formate and methyl acetate submechanisms. As another example, reaction mechanisms for methyl and ethyl propanoate

$CH_3O(C=O)CH_2CH_3$ and $CH_3CH_2O(C=O)CH_2CH_3$

should have the same H atom abstraction rates for the CH_3O- and CH_3CH_2O- portions of those molecules as those developed above. Only the H atom abstraction rates from the propanoate -$O(C=O)CH_2CH_3$ group would be needed as new information, and those rates should be expected to be the same in both methyl and ethyl propanoate. The present approach can also make mechanism development simpler in cases where the hydrocarbon segment is unsaturated, such as methyl crotonate [20] or methyl and ethyl propenoate.

ACKNOWLEDGMENTS

The computational portions of this work were supported by the U.S. Department of Energy, Office of Basic Energy Sciences, under the auspices of the U.S. Department of Energy by Lawrence Livermore National Laboratory under Contract DE-AC52-07NA27344. The experimental work was supported by the Division of Chemical Sciences, Geosciences and Biosciences, Office of Basic Energy Sciences U.S. Department of Energy; by the Chemical Sciences Division, Army Research Office; by the Deutsche Forschungsgemeinschaft KO 1363/18-3; and by the Sandia Corporation, a Lockheed Martin Company, for the National Nuclear Security Administration under contract DE-AC04-94-SL85000.

REFERENCES

1. M. S. Graboski and R. L. McCormick., Prog. Ener. Combust. Sci. 24 (1998) 125-164.

2. N. Miyamoto, H. Ogawa, N. M. Nurun, K. Obata, and T. Arima, Society of Automotive Engineers paper SAE-980506 (1998).

3. C. K. Westbrook, W. J. Pitz, and H. J. Curran, J. Phys. Chem. A 110 (2006) 6912-6922.

4. O. Herbinet, W. J. Pitz and C. K. Westbrook, Combust. Flame, submitted (2007).

5. E. M. Fisher, W. J. Pitz, H. J. Curran, and C. K. Westbrook, Proc. Combust. Inst. 28 (2000) 1579-1586.

6. S. Gaïl, M. J. Thomson, S. M. Sarathy, S.A. Syed, P. Dagaut, P. Dievart, A. J. Marchese and F. L. Dryer, Proc. Combust. Inst. 31 (2007) 305-311.

7. W. K. Metcalfe, S. Dooley, H. J. Curran, J. M. Simmie, A. M. El-Nahas and M. V. Navarro, J. Phys. Chem. A 111(19) (2007) 4001-4014.

8. L. Gasnot, V. Decottignies, and J. F. Pauwels, Fuel 84 (2005) 505-518.

9. P. Dagaut, N. Smoucovit and M. Cathonnet, Combust. Sci. Technol.127 (1997) 275-291.

10. P. Osswald, U. Struckmeier, T. Kasper, K. Kohse-Höinghaus, J. Wang, T. A. Cool, N. Hansen, and P. R. Westmoreland, J. Phys. Chem. A 111 (19) (2007) 4093-4101.

11. B. Yang, J. Wang, T. A. Cool, A. Lucassen, P. Osswald, U. Struckmeier, K. Kohse-Höinghaus, T. Kasper, N. Hansen, and P. R. Westmoreland, in preparation (2007).

12. D. Archambault and F. Billaud, J. Chim. Phys. 96 (1999) 778-796.

13. D. A. Good and J. S. Francisco, J. Phys. Chem. A 104 (2000) 1171-1185.

14. A. M. El-Nahas, M. V. Navarro, J. M. Simmie, J. W. Bozzelli, H. J. Curran, S. Dooley, and W. Metcalfe, J. Phys. Chem. A 111 (19) (2007) 3727-3739.

15. H. E. O'Neal and S. W. Benson, J. Phys. Chem. 71 (9) (1967) 2903-2921.

16. R. J. Kee, F. Rupley, J. A. Miller, et al., Chemkin Collection, Release 4.0, Reaction Design, Inc., 2007.

17. E. L. Petersen, D. M. Kalitan, S. Simmons, G. Bourque, H. J. Curran, and J. M. Simmie, Proc. Combust. Inst. 31 (2007) 447-454.

18. W. J. Pitz, C. V. Naik, T. N. Mhaolduin, C. K. Westbrook, H. J. Curran, J. P. Orme, and J. M. Simmie, Proc. Combust. Inst. 31 (2007) 267-275.

19. R. Sumathi and W. H. Green, Phys. Chem. Chem. Phys. 5 (16) (2003) 3402-3417.

20. S. M. Sarathy, S. Gail, S. A. Syed, M. J. Thomson, and P. Dagaut, Proc. Combust. Inst. 31 (1) (2007) 1015-1022.

Table 1
Flow conditions for ester flames in this study

Fuel	MA	EA	MF	EF
Pressure (torr)	30	30	30	30
Equiv. ratio	1.82	1.56	1.83	1.83
C/O	0.514	0.475	0.477	0.514
Inlet vel (cm/s)	64.0	65.7	66.6	64.0
Fuel slm	0.994	0.686	1.462	0.998
O2 slm	1.909	2.200	1.600	1.909
Ar slm	1.000	1.120	1.000	1.000

FIGURE CAPTIONS

1. Methyl and ethyl esters included in this study

2. Schematic of molecular elimination reaction pathways for ethyl formate and ethyl acetate

3. Fuel and major products in methyl formate flame. Circles are H_2O, diamonds are CO and fuel, squares are CO_2, triangles are H_2. Lines are computed values.

4. Computed results for ethene (solid line) and acetylene (dashed line), experimental values for ethene (circles) and acetylene (squares)

5. Computed results for formaldehyde (solid line) and formyl (dashed line), experimental values for formaldehyde (circles) and formyl (squares). Values for formyl have been increased by 10 for comparison.

6. Computed results for ketene (solid line) and propyne (dashed line), experimental values for ketene (circles) and propyne (squares). Values for propyne have been increased by 10 for comparison.

7. Computed results for methane (solid line) and acetaldehyde (dashed line), experimental values for methane (circles) and acetaldehyde (squares)

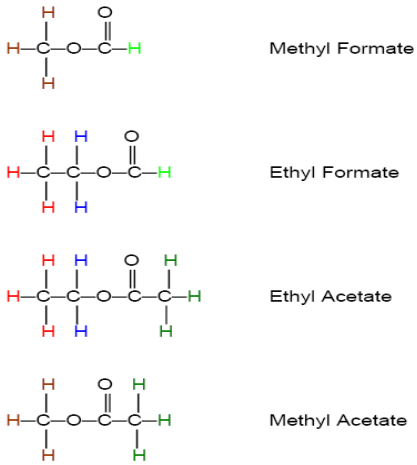

Figure 1 Methyl and ethyl esters included in this study

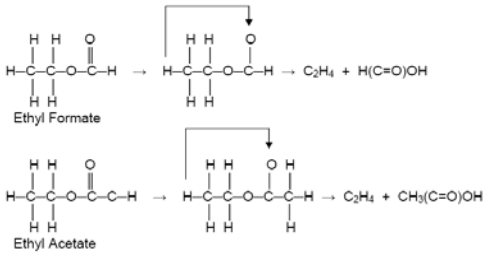

Figure 2 Schematic of molecular elimination reaction pathways for ethyl formate and ethyl acetate

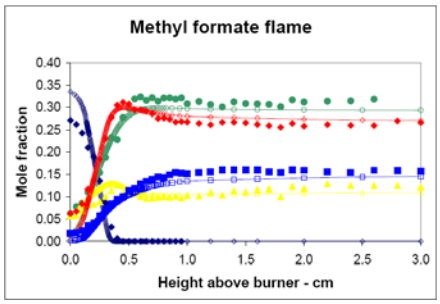

Fig. 3 Fuel and major products in methyl formate flame. Circles are H_2O, diamonds are CO and fuel, squares are CO_2, triangles are H_2. Lines are computed values.

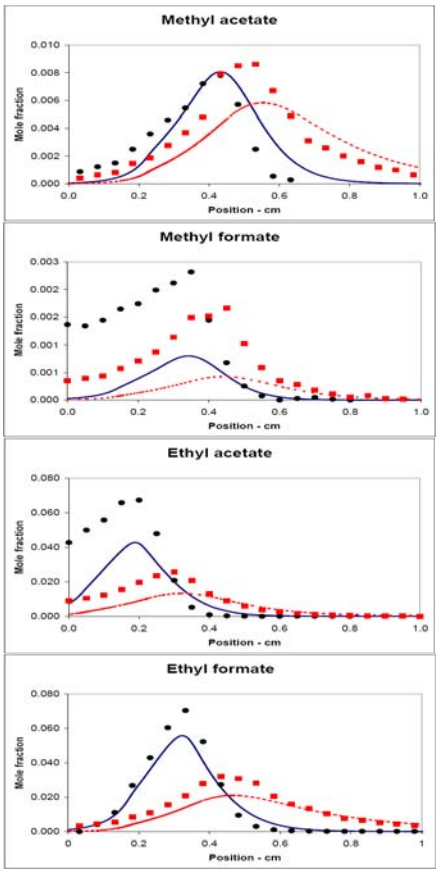

Fig. 4 Computed results for ethene (solid line) and acetylene (dashed line), experimental values for ethene (circles) and acetylene (squares)

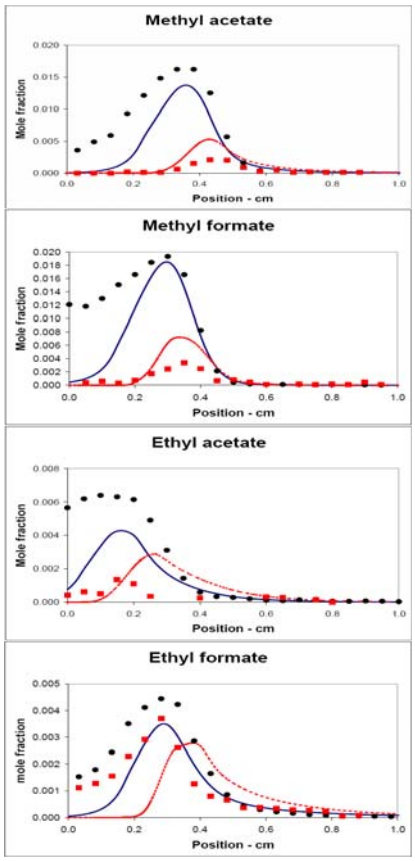

Fig. 5 Computed results for formaldehyde (solid line) and formyl (dashed line), experimental values for formaldehyde (circles) and formyl (squares). Values for formyl have been increased by 10 for comparison.

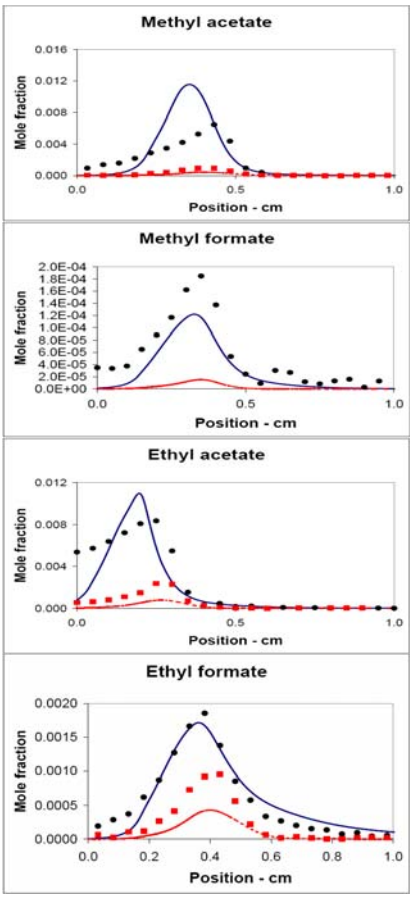

Fig 6 Computed results for ketene (solid line) and propyne (dashed line), experimental values for ketene (circles) and propyne (squares). Values for propyne have been increased by 10 for comparison.

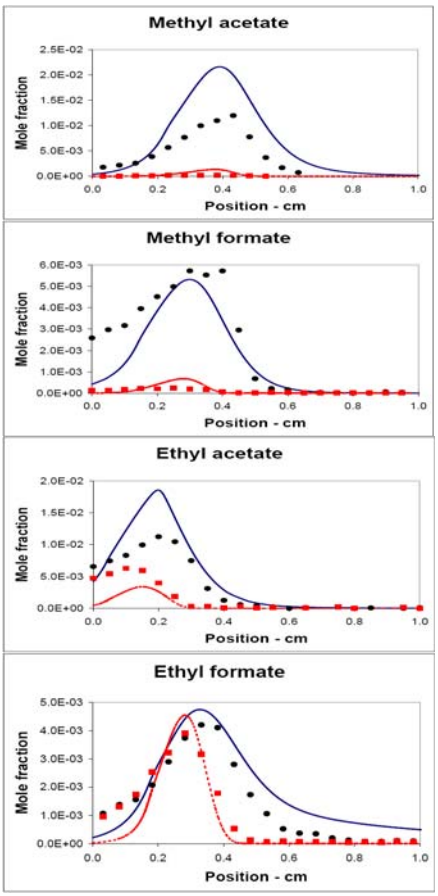

Fig 7 Computed results for methane (solid line) and acetaldehyde (dashed line), experimental values for methane (circles) and acetaldehyde (squares)

Supplemental material for (Westbrook et al., A Detailed Chemical Kinetic Reaction Mechanism for Oxidation of Four Small Alkyl Esters in Laminar Premixed Flames, Proc. Combust. Inst. 32, 2008)

Table S1

Arrhenius parameters for oxidation of Ethyl Formate (EF), Methyl Acetate (MA), Ethyl Acetate (EA) and Methyl Formate (MF). Units are mole, cm, sec, Kelvin, calories.

Reaction	A	n	Ea
EF+h=EFp+h2	1.88E+05	2.8	6280.0
EF+o2=EFp+ho2	2.00E+13	0.0	47500.0
EF+o=EFp+oh	1.03E+14	0.0	7850.0
EF+oh=EFp+h2o	1.05E+10	1.0	1586.0
EF+ho2=EPp+h2o2	1.68E+13	0.0	20430.0
EF+ch3=EFp+ch4	1.29E+12	0.0	11600.0
EF+c2h3=EFp+c2h4	1.00E+11	0.0	10400.0
EF+c2h5=EFp+c2h6	1.00E+11	0.0	10400.0
EF+ch3o=EFp+ch3oh	3.00E+11	0.0	7000.0
EF+ch3o2=EFp+ch3o2h	1.70E+13	0.0	20460.0
EFp=c2h4+ocho	1.34E+13	-0.4	24610.0
EF+o2=EFs+ho2	4.00E+13	0.0	47500.0
EF+h=EFs+h2	3.25E+05	2.4	4471.0
EF+o=EFs+oh	2.81E+13	0.0	5200.0
EF+oh=EFs+h2o	1.16E+07	1.6	-35.0
EF+ho2=EFs+h2o2	5.60E+12	0.0	17700.0
EF+ch3=EFs+ch4	3.98E+11	0.0	9500.0
EF+c2h3=EFs+c2h4	1.00E+11	0.0	10400.0
EF+c2h5=EFs+c2h6	1.00E+11	0.0	10400.0
EF+ch3o=EFs+ch3oh	3.00E+11	0.0	7000.0
EF+ch3o2=EFs+ch3o2h	2.00E+12	0.0	17000.0
EFs=ch3cho+hco	4.17E+15	-0.9	14040.0
EF+h=EFf+h2	6.50E+05	2.4	4471.0
EF+o=EFf+oh	5.51E+05	2.5	2830.0
EF+oh=EFf+h2o	2.33E+07	1.6	-35.0
EF+ch3=EFf+ch4	1.51E+00	3.5	5481.0
EF+ho2=EFf+h2o2	9.64E+03	2.6	13910.0
EF+o2=EFf+ho2	2.00E+13	0.0	49700.0
EF+ch3o=EFf+ch3oh	5.48E+11	0.0	5000.0
EF+ch3o2=EFf+ch3o2h	4.82E+03	2.6	13910.0
c2h5+co2=EFf	4.76E+07	1.5	37410.0
c2h5o+co=EFf	1.55E+06	2.0	5734.0
EFp+h=EF	1.00E+13	0.0	0.0
EFs+h=EF	1.00E+13	0.0	0.0
EFf+h=EF	1.00E+13	0.0	0.0
ocho+c2h5=EF	1.00E+12	0.0	0.0
hco+c2h5o=EF	1.00E+12	0.0	0.0
EF=hocho+c2h4	1.00E+13	0.0	50000.0
MA+h=MA1+h2	1.50E+05	2.4	2583.0
MA+o=MA1+oh	9.50E+04	2.4	1140.0
MA+oh=MA1+h2o	1.40E+10	0.5	63.0

```
MA+ch3=MA1+ch4                  1.50E-10    6.4      893.0
MA+ho2=MA1+h2o2                 9.00E+02    2.5    10532.0
MA+o2=MA1+ho2                   2.50E+12    0.0    48200.0
MA+ch3o=MA1+ch3oh               2.30E+10    0.0     2873.0
MA+ch3o2=MA1+ch3o2h             3.61E+03    2.5    10532.0
ch2co+ch3o=MA1                  5.00E+11    0.0    -1000.0
MA+h=MA2+h2                     9.40E+04    2.8     6280.0
MA+o=MA2+oh                     9.80E+05    2.4     4750.0
MA+oh=MA2+h2o                   5.25E+09    1.0     1590.0
MA+ch3=MA2+ch4                  4.52E-01    3.6     7154.0
MA+ho2=MA2+h2o2                 4.04E+04    2.5    16690.0
MA+o2=MA2+ho2                   3.00E+13    0.0    52000.0
MA+ch3o=MA2+ch3oh               1.58E+11    0.0     7000.0
MA+ch3o2=MA2+ch3o2h             2.38E+04    2.5    16490.0
MA+c2h3=EAm+c2h4                1.00E+11    0.0    10400.0
MA+c2h5=EAm+c2h6                1.00E+11    0.0    10400.0
ch2o+ch3co=MA2                  5.00E+11    0.0    -1000.0
ch3+ch3oco=MA                   1.81E+13    0.0        0.0
ch3co+ch3o=MA                   3.00E+13    0.0        0.0
ch3co2+ch3=MA                   3.00E+13    0.0        0.0
MA1+h=MA                        1.00E+13    0.0        0.0
MA2+h=MA                        1.00E+13    0.0        0.0

EA+h=EAp+h2                     1.88E+05    2.8     6280.0
EA+oh=EAp+h2o                   1.05E+10    1.0     1586.0
EA+o=EAp+oh                     1.03E+14    0.0     7850.0
EA+o2=EAp+ho2                   2.00E+13    0.0    47500.0
EA+ho2=EAp+h2o2                 1.68E+13    0.0    20430.0
EA+ch3=EAp+ch4                  1.29E+12    0.0    11600.0
EA+c2h3=EAp+c2h4                1.00E+11    0.0    10400.0
EA+c2h5=EAp+c2h6                1.00E+11    0.0    10400.0
EA+ch3o=EAp+ch3oh               3.00E+11    0.0     7000.0
EA+ch3o2=EAp+ch3o2h             1.70E+13    0.0    20460.0
EAp=c2h4+ch3co2                 1.34E+13   -0.4    24610.0
EA+h=EAs+h2                     3.25E+05    2.4     4471.0
EA+oh=EAs+h2o                   1.16E+07    1.6      -35.0
EA+o=EAs+oh                     2.81E+13    0.0     5200.0
EA+o2=EAs+ho2                   4.00E+13    0.0    47500.0
EA+ho2=EAs+h2o2                 5.60E+12    0.0    17700.0
EA+ch3=EAs+ch4                  3.98E+11    0.0     9500.0
EA+c2h3=EAs+c2h4                1.00E+11    0.0    10400.0
EA+c2h5=EAs+c2h6                1.00E+11    0.0    10400.0
EA+ch3o=EAs+ch3oh               3.00E+11    0.0     7000.0
EA+ch3o2=EAs+ch3o2h             2.00E+12    0.0    17000.0
EAs=ch3cho+ch3co                4.17E+15   -0.9    14040.0
EA+h=EAm+h2                     1.50E+05    2.4     2583.0
EA+oh=EAm+h2o                   1.40E+10    0.5       63.0
EA+o=EAm+oh                     9.50E+04    2.4     1140.0
EA+o2=EAm+ho2                   2.50E+12    0.0    48200.0
EA+ho2=EAm+h2o2                 9.00E+02    2.5    10532.0
EA+ch3=EAm+ch4                  1.50E-10    6.4      893.0
EA+c2h3=EAm+c2h4                1.00E+11    0.0    10400.0
EA+c2h5=EAm+c2h6                1.00E+11    0.0    10400.0
EA+ch3o=EAm+ch3oh               2.30E+10    0.0     2873.0
EA+ch3o2=EAm+ch3o2h             3.61E+03    2.5    10532.0
ch2co+c2h5o=EAm                 5.00E+11    0.0    -1000.0
EAp+h=EA                        1.00E+13    0.0        0.0
```

```
EAs+h=EA                          1.00E+13    0.0        0.0
EAm+h=EA                          1.00E+13    0.0        0.0
c2h5o+ch3co=EA                    3.00E+13    0.0        0.0
c2h5+ch3co2=EA                    3.00E+13    0.0        0.0
c2h5oco+ch3=EA                    3.00E+13    0.0        0.0
EA=ch3cooh+c2h4                   2.00E+13    0.0    50000.0

MF=ch2ocho+h                      8.24E+19   -1.1   102500.0
MF=ch3oco+h                       1.32E+19   -1.0   100100.0
MF=ch3oh+co                       1.00E+14    0.0    62500.0
MF=ch3o+hco                       5.37E+16    0.0    97090.0
MF=ch3+ocho                       3.21E+17   -0.5    79970.0
MF+o2=ch3oco+ho2                  2.00E+13    0.0    49700.0
MF+o2=ch2ocho+ho2                 3.00E+13    0.0    52000.0
MF+oh=ch3oco+h2o                  2.33E+07    1.6      -35.0
MF+oh=ch2ocho+h2o                 5.25E+09    1.0     1590.0
MF+ho2=ch3oco+h2o2                9.64E+03    2.6    13910.0
MF+ho2=ch2ocho+h2o2               4.04E+04    2.5    16690.0
MF+o=ch3oco+oh                    5.51E+05    2.5     2830.0
MF+o=ch2ocho+oh                   9.80E+05    2.4     4750.0
MF+h=ch3oco+h2                    6.50E+05    2.4     4471.0
MF+h=ch2ocho+h2                   9.40E+04    2.8     6280.0
MF+ch3=ch3oco+ch4                 1.51E+00    3.5     5481.0
MF+ch3=ch2ocho+ch4                4.52E-01    3.6     7154.0
MF+ch3o=ch3oco+ch3oh              5.48E+11    0.0     5000.0
MF+ch3o=ch2ocho+ch3oh             1.58E+11    0.0     7000.0
MF+ch3o2=ch3oco+ch3o2h            4.82E+03    2.6    13910.0
MF+ch3o2=ch2ocho+ch3o2h           2.38E+04    2.5    16490.0
MF+hco=ch3oco+ch2o                5.40E+06    1.9    17010.0
MF+hco=ch2ocho+ch2o               1.02E+05    2.5    18430.0
ch2ocho=ch3oco                    2.62E+11    0.0    38180.0
ch3oco=ch3+co2                    7.98E+12    0.3    15640.0
ch3oco=ch3o+co                    3.18E+13    0.5    23400.0
ch2ocho=ch2o+hco                  4.66E+12    0.1    27440.0
```